Int. J. Heat Mass Transfer. Vol. 23, pp. 819–831
Pergamon Press Ltd. 1980. Printed in Great Britain

BUOYANCY EFFECTS ON FLOW AND HEAT TRANSFER ON ROTATING AXISYMMETRIC ROUND-NOSED BODIES

ARYADI SUWONO
Department of Mechanical Engineering, Institute of Technology of Bandung, Bandung, Indonesia

(*Received* 10 *July* 1979)

Abstract — The paper presents a theoretical analysis of a steady laminar flow and heat transfer over rotating axisymmetric round-nosed bodies in which the effects of buoyancy force are taken into account. The solutions of the governing equations are expressed in terms of series expansion. The numerical computations are made for the case of rotating hemispheres, for $\lambda = Gr/Re^2$ ranging from 0 to ∞ and Prandtl numbers $Pr = 0.72$ and 100. For the opposing flow case, the numerical results are presented only for small values of λ. Using the results obtained for the hemispheres, the buoyancy-force effects on flow and heat transfer over a sphere are examined, including the effects on flow eruption.

NOMENCLATURE

$f, \tilde{f}$, reduced stream functions, defined in equations (13) and (39);
$g, \tilde{g}$, reduced stream functions, defined in equations (13) and (39);
g, acceleration due to gravity;
g_x, x-component of gravitational acceleration;
Gr, Grashof number, $g\beta\,|T_0 - T_\infty|\,L^3/\nu$;
$K(x)$, function of x denotes the sine of the angle between the acceleration vector and a normal to the surface of the body;
L, characteristic length;
Nu, Nusselt number, $gL/k(T_0 - T_\infty)$;
P, principal function, $\dfrac{2\xi}{\bar{r}}\dfrac{d\bar{r}}{d\xi}$;
Pr, Prandtl number, ν/α;
q, local wall heat flux;
Q, principal function, $\dfrac{2\xi K}{\bar{r}^5}$;
r, radial distance from a surface element to the axis of symmetry;
$\bar{r}$, dimensionless term of r, r/L;
Re, Reynolds number, U_oL/ν;
T, temperature;
$\bar{T}$, dimensionless temperature, $(T - T_\infty)/(T_0 - T_\infty)$;
u, velocity component in the x-direction;
$\bar{u}$, dimensionless term of u, u/U_c;
U_c, characteristic velocity;
v, velocity component in the y-direction;
$\bar{v}$, dimensionless normalizing term of v, $Re^{1/2}v/U_c$;
w, velocity component in rotating direction;
$\bar{w}$, dimensionless term of w, w/U_c;
x, coordinate, measured from stagnation point along the surface;
$\bar{x}$, dimensionless term of x, x/L;
y, coordinate, measured normal to x;
$\bar{y}$, dimensionless stretched term of y, $Re^{1/2}y/L$;
z, coordinate, measured in rotating direction;
$\bar{z}$, dimensionless term of z, z/L.

Greek symbols

α, thermal diffusivity;
β, thermal-expansion coefficient;
$\eta, \tilde{\eta}$, transformed coordinate, defined in equations (13) and (39);
$\theta, \tilde{\theta}$, dimensionless temperature, $(T - T_\infty)/(T_0 - T_\infty)$;
λ, dimensionless parameter, Gr/Re^2;
ν, kinematic viscosity;
$\xi, \tilde{\xi}$, transformed coordinate, defined in equations (13) and (39);
ω, angular velocity;
τ, wall frictional stress;
$\tilde{\tau}, \tilde{\tau}_x$, dimensionless term of the x-component of wall frictional stress, defined in equations (54) and (55);
$\tilde{\tau}_z, \tilde{\tau}_z$, dimensionless term of the z-component of wall frictional stress, defined in equations (54) and (55).

1. INTRODUCTION

WHEN a surface is in contact with a fluid whose temperature is different from the temperature of the surface, a non-uniform temperature is established in the fluid which can cause change in density. When the external force field is present in the fluid, this density changes, via the buoyant force, and may cause the fluid to move relative to the surface. When the fluid is also in motion relative to the surface induced by other means such as mechanical work, the buoyancy effects may influence the motion. For flows over submerged bodies, these effects are well known[1–8], but for flows engendered by rotating bodies, to the knowledge of the author, only the investigation of Kreith[9] on a rotating sphere where the surface temperature varies in special way admitting the similarity solutions to the momentum and energy equations, has dealt with the buoyancy effects.

The laminar boundary-layer flow and heat transfer

on rotating axisymmetric bodies in otherwise infinite undisturbed fluid have been treated by many investigators[10–15], and recently for a more general class of configurations by the author[16, 17], under the assumption that the effects of buoyant force can be neglected. However, the criterion to neglect the buoyancy effects for such flows is still unknown. It is the aim of the present paper to study the buoyancy effects on flow engendered by rotating axisymmetric bodies of uniform surface temperature. This study concerns round-nosed bodies, while the sharp-nosed bodies will be treated elsewhere. The difficulty of having a unified mathematical treatment is due to the non-similarity characteristic arising from the buoyant force-field, in addition to the non-similarity characteristic from the transverse curvature of the bodies.

To obtain the series solutions for the coupled momentum and energy equations, the coordinate transformation proposed by the author[16, 17] has been employed. The analysis is carried out for both assisting flow (in which the buoyancy force acts in the same direction as the forced flow) and opposing flow (in which the buoyancy force acts in the opposite direction to the forced flow). Finally, the series is applied to rotating hemispheres. The results for both assisting-flow and opposing-flow cases can be used to predict the velocity and temperature fields on rotating spheres. The influence of buoyancy forces on eruption of boundary-layer flow is also discussed.

2. DEVELOPMENT OF BASIC EQUATIONS

Consideration is hereby given to the steady, laminar boundary-layer flow over a rotating round-nosed body of revolution with uniform surface temperature T_0, situated in an infinite ambient fluid of undisturbed temperature T_∞ under a gravitational field which is parallel to the axis of rotation. Let x, y, and z be a non-rotating orthogonal curvilinear coordinate system with the corresponding velocity components u, v, and w, as shown in Fig. 1. If r is the radial distance from a surface element to the axis of symmetry, under the assumption of incompressible flow, negligible dissipation and constant properties (except the density changes which produce buoyancy forces), the governing boundary-layer equations are:

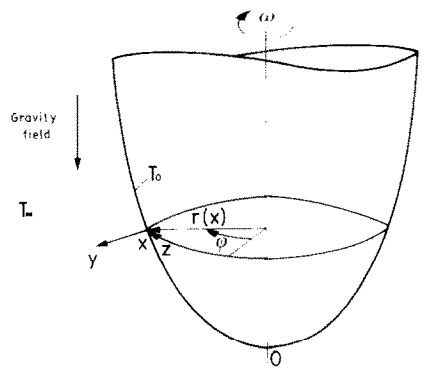

FIG. 1. The coordinate system.

$$\frac{\partial u}{\partial x}+\frac{\partial v}{\partial y}+\frac{u}{r}\frac{\mathrm{d}r}{\mathrm{d}x}=0, \tag{1}$$

$$u\frac{\partial u}{\partial x}+v\frac{\partial u}{\partial y}-\frac{w^2}{r}\frac{\mathrm{d}r}{\mathrm{d}x}=\nu\frac{\partial^2 u}{\partial y^2}\pm g_x\beta(T-T_\infty), \tag{2}$$

$$u\frac{\partial w}{\partial x}+v\frac{\partial w}{\partial y}+\frac{uw}{r}\frac{\mathrm{d}r}{\mathrm{d}x}=\nu\frac{\partial^2 w}{\partial y^2}, \tag{3}$$

$$u\frac{\partial T}{\partial x}+v\frac{\partial T}{\partial y}=\alpha\frac{\partial^2 w}{\partial y^2}. \tag{4}$$

Where β, ν, α and T are respectively, the thermal expansion coefficient, kinematic viscosity, thermal diffusivity, and temperature of the fluid. g_x is the x-component of the local gravitational-acceleration vector in the direction of increasing x. For convenience of further discussion, g_x will be written as

$$g_x=gK(x) \tag{5}$$

where g is a positive constant having the dimension of acceleration and $K(x)$ is a nondimensional function of x. In equation (2), the positive sign applies in the assisting flow, whereas the negative sign applies in the opposing flow. If the surface is faced downward, they correspond to the case $T_0>T_\infty$ and $T_0<T_\infty$, respectively.

$$\begin{gathered}u=v=0,\quad W=r\omega,\quad T=T_0\quad\text{at } y=0\\ u,w\to 0,\quad T\to T_\infty\quad\text{as } y\to\infty.\end{gathered} \tag{6}$$

The conservation equations can be recast into a dimensionless form by introducing a reference length L and a reference velocity U_c, the appropriate stretched coordinates, and the normalizing velocities and temperatures as defined below,

$$\begin{gathered}\bar{x}=x/L;\quad \bar{r}=r/L;\quad \bar{y}=Re^{1/2}y/L;\\ \bar{u}=u/U_c;\quad \bar{v}=Re^{1/2}v/U_c;\quad \bar{w}=w/U_c;\\ \bar{T}=(T-T_\infty)/(T_0-T_\infty)\end{gathered} \tag{7}$$

where the Reynolds number $Re=U_cL/\nu$. Accordingly, equations (1)–(4) become

$$\frac{\partial\bar{u}}{\partial\bar{x}}+\frac{\partial\bar{v}}{\partial\bar{y}}+\frac{\bar{u}}{\bar{r}}\frac{\mathrm{d}\bar{r}}{\mathrm{d}\bar{x}}=0, \tag{8}$$

$$\bar{u}\frac{\partial\bar{u}}{\partial\bar{x}}+\bar{v}\frac{\partial\bar{u}}{\partial\bar{y}}-\frac{w^2}{\bar{r}}\frac{\mathrm{d}\bar{r}}{\mathrm{d}\bar{x}}=\frac{\partial^2\bar{u}}{\partial\bar{y}^2}\pm\frac{Gr}{Re^2}K(\bar{x})\bar{T}, \tag{9}$$

$$\bar{u}\frac{\partial\bar{w}}{\partial\bar{x}}+\bar{v}\frac{\partial\bar{w}}{\partial\bar{y}}+\frac{\bar{u}\bar{w}}{\bar{r}}\frac{\mathrm{d}\bar{r}}{\mathrm{d}\bar{x}}=\frac{\partial^2\bar{w}}{\partial\bar{y}^2}, \tag{10}$$

$$\bar{u}\frac{\partial\bar{T}}{\partial\bar{y}}+\bar{v}\frac{\partial\bar{T}}{\partial\bar{y}}=Pr^{-1}\frac{\partial^2\bar{T}}{\partial\bar{y}^2}, \tag{11}$$

where Pr and Gr denote, respectively, the Prandtl number ν/α, and the Grashof number, $g\beta|T_0-T_\infty|L^3/\nu$. If $L\omega$ is chosen as the reference velocity, the boundary conditions are then

$$\begin{gathered}\bar{u}=\bar{v}=0;\quad \bar{w}=\bar{r};\quad \bar{T}=1\quad\text{at } \bar{y}=0,\\ \bar{u},\bar{w}\to 0;\quad T\to 0\quad\text{as } \bar{y}\to\infty.\end{gathered} \tag{12}$$

The next step in the analysis is the transformation from $(\bar{x}, \bar{y})$ coordinates to (ξ, η) coordinates. The recent investigations of the author[16, 17] for the prediction of pure forced-convection boundary-layer transfer suggest the following transformation of variables.

$$\xi = \int_0^{\bar{x}} [\bar{r}(\bar{x})]^3 \mathrm{d}\bar{x}; \quad \eta = \frac{\bar{r}^2}{(2\xi)^{1/2}} \bar{y};$$

$$f(\xi, \eta) = \frac{\psi(\bar{x}, \bar{y})}{(2\xi)^{1/2}}; \quad g(\xi, \eta) = \frac{r\phi(\bar{x}, \bar{y})}{(2\xi)^{1/2}}; \tag{13}$$

$$\theta(\xi, \eta) = \bar{T}(\bar{x}, \bar{y})$$

where $\psi(\bar{x}. \bar{y})$ and $\phi(\bar{x}, \bar{y})$ are dimensionless stream functions, satisfy the continuity equation with

$$\bar{u} = \frac{1}{\bar{r}} \frac{\partial \psi}{\partial \bar{y}}; \quad \bar{v} = -\frac{1}{\bar{r}} \frac{\partial \psi}{\partial \bar{x}}; \quad \bar{w} = \frac{\partial \phi}{\partial \bar{y}}. \tag{14}$$

In terms of the new variables, the dimensionless velocity components become

$$\bar{u} = \bar{r} f', \tag{15}$$

$$\bar{v} = -\frac{\bar{r}^2}{(2\xi)^{1/2}} \left[f + 2\xi \frac{\partial f}{\partial \xi} + \eta f'(2P(\xi) - 1) \right], \tag{16}$$

$$\bar{w} = \bar{r} g' \tag{17}$$

where

$$P(\xi) = \frac{2\xi}{\bar{r}} \frac{\mathrm{d}\bar{r}}{\mathrm{d}\xi}. \tag{18}$$

In equations (15)–(17) and other equations which follow, the primes denote partial differentiation with respect to η. Using the foregoing transformations, the momentum equations (9) and (10) and the energy equation (11) become, respectively,

$$f''' + ff'' - P(\xi)(f'^2 - g'^2) \pm \lambda Q(\xi)\theta = 2\xi \frac{\partial(f', f)}{\partial(\xi, \eta)}, \tag{19}$$

$$g''' + fg'' - 2P(\xi) f'g' = 2\xi \frac{\partial(g', f)}{\partial(\xi, \eta)}, \tag{20}$$

$$Pr^{-1}\theta'' + f\theta' = 2\xi \frac{\partial(\theta, f)}{\partial(\xi, \eta)} \tag{21}$$

where

$$\lambda = \frac{Gr}{Re^2}; \quad Q(\xi) = \frac{2\xi K(\xi)}{\bar{r}^5}, \tag{22}$$

with the boundary conditions

$$f = f' = 0; \quad g = \theta = 1 \quad \text{at } \eta = 0$$

$$f', g', \theta \to 0 \quad \text{as } \eta \to \infty. \tag{23}$$

For the case $\lambda = 0$, equations (19)–(21) reduce to the equations of pure-convection boundary-layer transfer where the solutions may be found in[16, 17].

As in[16, 17], to obtain the series solutions, Görtler's terminology of principal function for $P(\xi)$ and $Q(\xi)$, will be employed in the present analysis. The round-nosed bodies under consideration are supposed to have the following expansion form

$$r(x) = x \sum_{n=0}^{\infty} r_n x^{2n}. \tag{24}$$

Upon selecting r_0 as the reference length L, and since

$$\frac{\mathrm{d}r}{\mathrm{d}x} = [1 - (K(x))^2]^{1/2} \tag{25}$$

it follows that

$$K(\bar{x}) = \bar{x} \sum_{n=0}^{\infty} K_n \bar{x}^{2n} \tag{26}$$

where $K_0 = 1$, and for $n > 0$ K_n depend on $r_0, r_1, \ldots, r_n$. Accordingly, the principal functions $P(\xi)$ can be expanded as the following sereis

$$P(\xi) = \tfrac{1}{2} + \sum_{n=1}^{\infty} P_n \xi^{n/2}; \quad Q(\xi) = \tfrac{1}{2} + \sum_{n=1}^{\infty} Q_n \xi^{n/2}. \tag{27}$$

The dependence of P_n on $r_0, r_1, \ldots, r_n$ will be understood implicitly.

Now, having shown the form of the expansion for the principal functions, we introduce the following expansion for the other dependent variables

$$f(\xi, \eta) = \sum_{n=0}^{\infty} f_n(\eta)\xi^{n/2}; \quad g(\xi, \eta) = \sum_{n=0}^{\infty} g_n(\eta)\xi^{n/2};$$

$$\theta(\xi, \eta) = \sum_{n=0}^{\infty} \theta_n(\eta)\xi^{n/2}. \tag{28}$$

Substitution of these expansion forms into equations (19)–(21), followed by collecting terms common to equal power of ξ, we obtain a sequence of coupled sets of ordinary differential equations. We have, for $n = 0$

$$f_0''' + f_0 f_0'' - \tfrac{1}{2}(f_0'^2 - g_0'^2) \pm \frac{\lambda}{2}\theta_0 = 0, \tag{29}$$

$$g_0''' + f_0 g_0'' - f_0' g_0' = 0, \tag{30}$$

$$Pr^{-1}\theta_0'' + f_0\theta_0' = 0 \tag{31}$$

and for $n > 0$

$$f_n''' + f_0 f_n'' - (n+1) f_0' f_n' + (n+1) f_0'' f_n + g_0' g_n' \pm \frac{\lambda}{2}\theta_n = L_{n-1}, \tag{32}$$

$$g_n''' + f_0 g_n'' - (n+1) f_0' g_n' + g_0' f_n' + (n+1) g_0'' f_n = M_{n-1}, \tag{33}$$

$$Pr^{-1}\theta_n'' + f_0\theta_n' - n f_0'\theta_n + (n+1)\theta_0' f_n = N_{n-1} \tag{34}$$

where L_{n-1}, M_{n-1}, and N_{n-1} are defined by

$$L_{n-1} = P_n(f_0'^2 - g_0'^2) \pm \lambda Q_n\theta_0 + \sum_{m=1}^{n-1} [P_m(f_0' f_{n-m}' - g_0' g_{n-m}')$$

$$+ (m+\tfrac{1}{2}) f'_m f'_{n-m} - \tfrac{1}{2} g'_m g'_{n-m} - (m+1) f_m f''_{n-m} \pm \lambda Q_m \theta_{n-m}]$$

$$+ \sum_{m=1}^{n-1} \sum_{i=1}^{n-m} P_m (f'_i f'_{n-m-i} - g_i g_{n-m-i}), \quad (35)$$

$$M_{n-1} = 2P_n f'_0 g'_0 + \sum_{m=1}^{n-1} [2P_m g'_0 f'_{n-m} + (m+1) g'_m f'_{n-m} - (m+1) f_m g''_{n-m}] + \sum_{m=1}^{n-1} \sum_{i=1}^{n-m} 2P_m g'_i f'_{n-m-i} \quad (36)$$

$$N_{n-1} = \sum_{m=1}^{n-1} [m\theta_m f'_{n-m} - (m+1) f_m \theta'_{n-m}]. \quad (37)$$

The boundary conditions are

$$\begin{aligned} &f_0 = f'_0 = 0; \quad g'_0 = \theta_0 = 1; \\ &f_n = f'_n = g'_n = \theta_n = 0 \quad \text{at } \eta = 0; \\ &f'_n, g'_n, \theta_n \to 0 \quad \text{as } \eta \to \infty; \end{aligned} \quad (38)$$

For systems with ratio $\lambda = (Gr/R_e^2)$ large, it is more convenient to use $1/\lambda$ as an integration parameter. For this purpose, we introduce the following new variables

$$\tilde{\xi} = \xi; \quad \tilde{\eta} = \lambda^{1/4}\eta; \quad \tilde{f}(\tilde{\xi}, \tilde{\eta}) = \frac{f(\xi, \eta)}{\lambda^{1/4}};$$
$$\tilde{g}(\tilde{\xi}, \tilde{\eta}) = \lambda^{1/4} g(\xi, \eta); \quad \tilde{\theta}(\tilde{\xi}, \tilde{\eta}) = \theta(\xi, \eta). \quad (39)$$

In terms of the new variables, equations (19)–(21) become, after transformation,

$$\tilde{f}''' + \tilde{f}\tilde{f}'' - P(\tilde{\xi})(\tilde{f}'^2 - \lambda^{-1}\tilde{g}'^2) \pm Q(\tilde{\xi})\tilde{\theta} = 2\tilde{\xi}\frac{\partial(\tilde{f}', \tilde{f})}{\partial(\tilde{\xi}, \tilde{\eta})}, \quad (40)$$

$$\tilde{g}''' + \tilde{f}\tilde{g}'' - 2P(\tilde{\xi})\tilde{f}'\tilde{g}' = 2\tilde{\xi}\frac{\partial(\tilde{g}', \tilde{f})}{\partial(\tilde{\xi}, \tilde{\eta})}, \quad (41)$$

$$Pr^{-1}\tilde{\theta}'' + \tilde{f}\tilde{\theta}' = 2\tilde{\xi}\frac{\partial(\tilde{\theta}, \tilde{f})}{\partial(\tilde{\xi}, \tilde{\eta})} \quad (42)$$

with

$$\tilde{f} = \tilde{f}' = 0; \quad \tilde{g} = \tilde{\theta} = 1 \quad \text{at } \tilde{\eta} = 0,$$
$$\tilde{f}', \tilde{g}', \tilde{\theta} \to 0 \quad \text{as } \tilde{\eta} \to \infty. \quad (43)$$

For $\lambda \to \infty$, all terms containing $\tilde{g}'$, $\tilde{g}''$ and $\tilde{g}'''$ vanish. It is seen that equations (40) and (42) are similar to those of Lin and Chao[18] in their study of boundary-layer transfer in free convection.

Using the same procedure as for the case of small λ, we can obtain the ordinary differential equations for functional coefficients when the new dependent variables are expanded similar to that of (28). They are

$$\tilde{f}'''_0 + \tilde{f}_0\tilde{f}''_0 - \tfrac{1}{2}(\tilde{f}'^2_0 - \lambda^{-1}\tilde{g}'^2_0) \pm \tfrac{1}{2}\tilde{\theta}_0 = 0, \quad (44)$$

$$\tilde{g}'''_0 + \tilde{f}_0\tilde{g}''_0 - \tilde{f}'_0\tilde{g}'_0 = 0, \quad (45)$$

$$Pr^{-1}\tilde{\theta}''_0 + \tilde{f}_0\tilde{\theta}'_0 = 0 \quad (46)$$

and

$$\tilde{f}'''_n + \tilde{f}_0\tilde{f}''_n - (n+1)\tilde{f}'_0\tilde{f}'_n + \lambda^{-1}\tilde{g}'_0\tilde{g}'_n \pm \tfrac{1}{2}\tilde{\theta}_n = \tilde{L}_{n-1}, \quad (47)$$

$$\tilde{g}'''_n + \tilde{f}_0\tilde{g}''_n - (n+1)\tilde{f}'_0\tilde{g}'_n + \tilde{g}'_0\tilde{f}'_n + (n+1)\tilde{g}''_0\tilde{f}_n = \tilde{M}_{n-1}, \quad (48)$$

$$Pr^{-1}\tilde{\theta}''_n + \tilde{f}_0\tilde{\theta}'_n - n\tilde{f}'_0\tilde{\theta}_n + (n+1)\tilde{\theta}'_0\tilde{f}_n = N_{n-1}, \quad (49)$$

where

$$\tilde{L}_{n-1} = P_n(\tilde{f}'^2_0 - \lambda^{-1}\tilde{g}'^2_0) \pm Q_n\tilde{\theta}_0 + \sum_{m=1}^{n-1} [P_m(\tilde{f}'_0 f'_{n-m} - \lambda^{-1}\tilde{g}'_0\tilde{g}'_{n-m}) + (m+\tfrac{1}{2})\tilde{f}'_m\tilde{f}'_{n-m} - \frac{\lambda^{-1}}{2}\tilde{g}'_m\tilde{g}'_{n-m} - (m+1)\tilde{f}_m\tilde{f}''_{n-m} \pm Q_m\tilde{\theta}_{n-m}] + \sum_{m=1}^{n-1}\sum_{i=1}^{n-m} P_m[\tilde{f}'_i\tilde{f}'_{n-m-i} - \lambda^{-1}\tilde{g}'_i\tilde{g}'_{n-m-i}], \quad (50)$$

$$\tilde{M}_{n-1} = 2P_n\tilde{f}'_0\tilde{g}'_0 + \sum_{m=1}^{n-1} [2P_m\tilde{g}'_0\tilde{f}'_{n-m} + (m+1)\tilde{g}'_m\tilde{f}'_{n-m} - (m+1)\tilde{f}_m\tilde{g}''_{n-m}] + \sum_{m=1}^{n-1}\sum_{i=1}^{n-m} 2P_m\tilde{g}'_i\tilde{f}'_{n-m-i}, \quad (51)$$

$$\tilde{N}_{n-1} = \sum_{m=1}^{n-1} [m\tilde{\theta}_m\tilde{f}'_{n-m} - (m+1)\tilde{f}_m\tilde{\theta}'_{n-m}], \quad (52)$$

with the boundary conditions

$$\begin{aligned} &\tilde{f}_0 = \tilde{f}'_0 = 0; \quad \tilde{g}'_0 = \tilde{\theta}_0 = 1; \\ &\tilde{f}_n = \tilde{f}'_n = \tilde{\theta}_n = 0 \quad \text{at } \tilde{\eta} = 0 \\ &\tilde{f}'_0, \tilde{g}'_0, \tilde{\theta}_0 \to 0; \quad \tilde{f}'_n, \tilde{g}'_n, \tilde{\theta}_n \to 0 \quad \text{as } \tilde{\eta} \to \infty. \end{aligned} \quad (53)$$

3. WALL FRICTIONAL-STRESS AND WALL HEAT-FLUX

In technological applications, it is often the wall frictional-stress and wall heat-flux that are of the greatest interest. In dimensionless terms, the components of local frictional stress for small values of λ are given by

$$\bar{\tau}_x = \frac{\tau_x Re^{1/2}}{\rho(L\omega)^2} = \frac{\bar{r}^3}{(2\xi)^{1/2}} \sum_{n=0}^{\infty} f''_n(0)\xi^{n/2};$$
$$\bar{\tau}_z = \frac{\tau_z Re^{1/2}}{\rho(L\omega)^2} = \frac{\bar{r}^3}{(2\xi)^{1/2}} \sum_{n=0}^{\infty} g''_n(0)\xi^{n/2}, \quad (54)$$

wherein ρ is the density of the fluid. In terms of the variables for large values of λ, they are

$$\tilde{\tau}_x = \frac{\tau_x Re^{1/2}}{\rho(L\omega)^2\lambda^{3/4}} = \frac{\bar{r}^3}{(2\tilde{\xi})^{1/2}} \sum_{n=0}^{\infty} \tilde{f}''_n(0)\tilde{\xi}^{n/2};$$
$$\tilde{\tau}_z = \frac{\tau_x Re^{1/2}}{\rho(L\omega)^2\lambda^{3/4}} = \frac{\bar{r}^3}{(2\xi)^{1/2}} \sum_{n=0}^{\infty} \tilde{g}''_n(0)\tilde{\xi}^{n/2}. \quad (55)$$

The torque created by the frictional stress at the wall can be obtained by integrating the z-component of local frictional stress over the surface. In dimensionless term, for small values of λ that is

$$\bar{M} = \frac{M\,Re^{1/2}}{\rho L^4 \omega^2} = 2\pi \int_0^{\bar{x}_m} \bar{r}^2 \bar{\tau}_z \mathrm{d}\bar{x} \tag{56}$$

where x_m is the maximum value of x for the body. And for large values of λ

$$\bar{M} = \frac{2\pi}{\lambda^{3/4}} \int_0^{\bar{x}_m} \bar{r}^2 \tilde{\tau}_z \mathrm{d}\bar{x}. \tag{57}$$

The local-wall heat-flux may be written in the form of a Nusselt number as

$$\frac{Nu}{Re^{1/2}} = \frac{qL}{Re^{1/2} k(T_0 - T_\infty)} = -\frac{\bar{r}^2}{(2\xi)^{1/2}} \sum_{n=0}^{\infty} \theta_n'(0) \xi^{n/2} \tag{58}$$

or

$$\frac{Nu}{Re^{1/2}} = \frac{qL}{Re^{1/2} k(T_0 - T_\infty)} = -\frac{\lambda^{1/4} \bar{r}^2}{(2\xi)^{1/2}} \sum_{n=0}^{\infty} \tilde{\theta}_n'(0) \xi^{n/2} \tag{59}$$

and k denotes the thermal conductivity of the fluid.

4. APPLICATION TO A ROTATING HEMISPHERE

As an example, in this section, we discuss the application of the results to the case of a rotating hemisphere. Under consideration is a hemisphere of radius R oriented parallel with respect to the gravitational vector g. Upon selecting R as the reference length L, the following relationships can be readily established:

$$\bar{r}(\bar{x}) = K(\bar{x}) = \sin \bar{x}, \tag{60}$$

$$\xi = \tilde{\xi} = \frac{\cos^3 \bar{x}}{3} - \cos \bar{x} + \frac{2}{3}, \tag{61}$$

$$P_1 = -\frac{1}{6}; \quad P_2 = -\frac{11}{72}; \quad P_3 = \frac{53}{432}, \tag{62}$$

$$Q_1 = \tfrac{1}{2}; \quad Q_2 = \frac{19}{72}; \quad Q_3 = \frac{2247}{22680}. \tag{63}$$

Using these values, the equations (29)–(34) with the boundary conditions (38) have been numerically integrated up to four terms following the Runge–Kutta–Merson (RKM) procedure for $Pr = 0.72$ and 100 and 11 values of small λ ranging from 0 to 1, and similarly for large values of λ, the parameters of integration being λ^{-1} ranging from 0 to 1. A tabulation of the appropriate wall derivatives of the functional coefficients are given in Tables 1 and 2. For the opposing-flow case, the numerical computations are made only for $\lambda = 0.1$ and $Pr = 1$ and 100 due to the difficulty caused by the fact that for sufficiently large values of λ, the shear stress at the wall will vanish. Under this condition the separation of boundary layers will occur and the classical boundary-layer analysis will cease to apply.

It should be noted that, for $\lambda = 0$ and $\lambda = \infty$, the results can be used to analyse the boundary-layer transfer on a rotating sphere for pure forced-convection and pure free-convection, respectively. For both cases, the results on Nusselt numbers agree with analytical studies made by other investigators (see for example [11, 14, 15, 17] for pure forced convection and [18, 19] for pure free convection).

Representative velocity profiles at selected axial locations $\bar{x} = \pi/6$, $\pi/3$, and $\pi/2$, for several parametric values λ are illustrated in Figs. 2 and 3 in which the dimensionless velocity components $\bar{u}$ and $\bar{w}$ are plotted against η to show the effects of buoyancy force on the boundary layer. It is seen that the flow boundary-layer thickness decreases as λ increases, and is accompanied by a relatively sharp rise in the velocity profiles. The temperature profiles at these three selected locations and for the same variation of parametric values λ are shown in Fig. 4. An inspection of the figure reveals that as the buoyancy force effect λ increases the temperature gradient at the wall increases but the thermal boundary-layer thickness decreases.

5. APPLICATION TO A ROTATING SPHERE

A major interest of the present investigation is in the analysis of the buoyancy-force effects on flow and thermal boundary-layer on a rotating sphere. When the axis of rotation is parallel to the direction of gravitational force, the buoyancy-force effects make the flow and thermal boundary-layer non-symmetric with respect to the equator. Hence, the analysis of the flow and thermal boundary-layer is different from that of pure forced-convective flow, or from that of pure natural-convective flow which has only one direction for the main flow.

For the present case, the determination of flow- and heat-transfer characteristic is to apply the results obtained for a hemisphere for both cases, the assisting and the opposing flow. The assisting-flow case should be applied to the lower part of the sphere, if the sphere is heated or the upper part if the sphere is cooled, whereas the opposing-flow case is applied to the upper part for the heated-surface case or the lower part for the case of cooled surface. It should be noted in the present case, that the validity region for application of the results is not symmetrical due to the displacement of the eruption point caused, by the buoyancy force effects. Thus, the first step, before the results of calculation for hemisphere are used, is to determine the point where the eruption occurs. As in the case of pure forced-convective flow, the eruption point of flow can be determined by finding the point where the x-component of local-wall frictional-stress has the same magnitude but with the opposite direction. For pure forced-convective flow, the eruption occurs at the equator. Figure 5 shows the plots of the x-component of local-wall frictional-stress on a sphere for pure forced-convective flow and for $\lambda = 0.1$ with Prandtl numbers $Pr = 1$ and 100 showing the effects of buoyancy force on flow eruption.

Table 1. Wall derivatives of functional coefficients for $Pr = 0.72$, 100 and λ ranging from 0 to 1

Pr	λ	$f_0''(0)$	$-f_1''(0)$	$-f_2''(0)$	$f_3''(0)$	$-g_0''(0)$	$g_1''(0)$	$g_2''(0)$	$-g_3''(0)$	$-\theta_0''(0)$	$\theta_1''(0)$	$\theta_2''(0)$	$-\theta_3''(0)$
$Pr = 0.72$	0.0	0.360789	0.083072	0.079550	0.048235	0.435523	0.036390	0.032988	0.027667	0.232336	0.016375	0.018837	0.006647
	0.1	0.404620	0.046376	0.050796	0.056987	0.466242	0.035632	0.031383	0.026823	0.254817	0.002584	0.003920	0.010398
	0.2	0.447642	0.014216	0.026437	0.062980	0.490999	0.035979	0.031375	0.025516	0.271439	− 0.013425	0.004036	0.010983
	0.3	0.489615	− 0.015045	0.004774	0.067672	0.512225	0.036576	0.031762	0.024375	0.285156	− 0.021168	− 0.009451	0.010784
	0.4	0.530574	− 0.042234	− 0.015043	0.071654	0.530982	0.037245	0.032282	0.023432	0.297005	− 0.027188	− 0.013509	0.010388
	0.5	0.570596	− 0.067844	− 0.033506	0.075208	0.547876	0.037928	0.032848	0.022658	0.307517	− 0.032103	− 0.016729	0.009823
	0.6	0.609763	− 0.092202	− 0.050925	0.078484	0.563301	0.038602	0.033421	0.022018	0.317011	− 0.036253	− 0.019389	0.009306
	0.7	0.648149	− 0.115544	− 0.067516	0.081568	0.577581	0.039240	0.033976	0.021484	0.325697	− 0.039859	− 0.021656	0.008812
	0.8	0.685821	− 0.138004	− 0.083405	0.084510	0.590766	0.039889	0.034536	0.021037	0.333723	− 0.043005	− 0.023612	0.008351
	0.9	0.722837	− 0.159741	− 0.098725	0.087349	0.603155	0.040497	0.035067	0.020657	0.341197	− 0.045832	− 0.025347	0.007924
	1.0	0.759248	− 0.180840	− 0.113551	0.090105	0.614819	0.041083	0.035578	0.020333	0.348204	− 0.048387	− 0.026900	0.007530
$Pr = 100$	0.0	0.360789	0.083072	0.079550	0.048235	0.435523	0.036390	0.032988	0.027667	1.900095	0.180150	0.200266	0.087656
	0.1	0.373476	0.070136	0.067983	0.050258	0.437435	0.037107	0.033378	0.027768	1.916137	0.158378	0.175519	0.099645
	0.2	0.386000	0.059963	0.059150	0.053405	0.439296	0.037285	0.033457	0.027682	1.931709	0.138084	0.153342	0.108955
	0.3	0.398371	0.050128	0.050802	0.056134	0.441109	0.037495	0.033549	0.027577	1.946845	0.119098	0.133337	0.116185
	0.4	0.410597	0.040599	0.042874	0.058530	0.442877	0.037629	0.033652	0.027458	1.961575	0.101278	0.115183	..121878
	0.5	0.422686	0.031345	0.035312	0.060658	0.444603	0.037795	0.033762	0.027332	1.975923	0.084501	0.098622	0.126101
	0.6	0.434645	0.022343	0.028071	0.062569	0.446289	0.037959	0.033879	0.027201	1.989913	0.068662	0.083437	0.129392
	0.7	0.446480	0.013572	0.021113	0.064302	0.447938	0.038119	0.034001	0.027068	2.003567	0.053673	0.069451	0.131862
	0.8	0.458199	0.005010	0.014408	0.065889	0.449551	0.038376	0.034126	0.026935	2.016904	0.039449	0.056516	0.133672
	0.9	0.449805	− 0.003357	0.007928	0.067354	0.451132	.038431	0.034253	0.026804	2.029940	0.025927	0.044507	0.134949
	1.0	0.481305	− 0.011544	0.001651	0.068718	0.452680	0.038582	0.034383	0.026674	2.042693	0.013043	0.033318	0.135791

Table 2. Wall derivatives of functional coefficients for $Pr = 0.72$, 100 and λ^{-1} ranging from 0 to 1

Pr	λ	$\tilde{f}_0''(0)$	$\tilde{f}_1''(0)$	$\tilde{f}_2''(0)$	$\tilde{f}_3''(0)$	$-\tilde{g}_0''(0)$	$\tilde{g}_1''(0)$	$\tilde{g}_2''(0)$	$-\tilde{g}_3''(0)$	$-\tilde{\theta}_0''(0)$	$-\tilde{\theta}_1''(0)$	$-\tilde{\theta}_2''(0)$	$\tilde{\theta}_3''(0)$
$Pr = 0.72$	0.0	0.540676	0.259850	0.177736	0.041420	0.569254	0.036485	0.032189	0.009892	0.326840	0.063066	0.035704	0.001280
	0.1	0.563617	0.251199	0.170968	0.047061	0.574369	0.037001	0.032533	0.011220	0.329217	0.061282	0.034728	0.000050
	0.2	0.586281	0.242746	0.164283	0.052486	0.579337	0.037503	0.032878	0.012469	0.331532	0.059583	0.033774	−0.001079
	0.3	0.608685	0.234477	0.157680	0.057715	0.584170	0.037991	0.033222	0.013645	0.333788	0.057964	0.032841	−0.002118
	0.4	0.630842	0.226380	0.151157	0.062767	0.588874	0.038466	0.033565	0.014756	0.335989	0.056417	0.031930	−0.003076
	0.5	0.652766	0.218443	0.144711	0.067657	0.593460	0.038929	0.033907	0.015808	0.338138	0.054938	0.031041	−0.003962
	0.6	0.674467	0.210657	0.138340	0.072398	0.597932	0.039380	0.034247	0.016805	0.340238	0.053521	0.030173	−0.004783
	0.7	0.695957	0.203011	0.132040	0.077004	0.602299	0.039821	0.034584	0.017752	0.342293	0.052161	0.029325	−0.005545
	0.8	0.717244	0.195498	0.125810	0.081483	0.606566	0.040251	0.034918	0.018653	0.344304	0.050854	0.028497	−0.006253
	0.9	0.738339	0.188111	0.119648	0.085848	0.610737	0.040672	0.035250	0.019513	0.346273	0.049598	0.027689	−0.006914
	1.0	0.759248	0.180840	0.113551	0.090105	0.614819	0.041083	0.035578	0.020333	0.348204	0.048387	0.026900	−0.007530
$Pr = 100$	0.0	0.197430	0.097290	0.067007	0.016865	0.242913	0.021261	0.020340	0.008342	1.402531	0.290196	0.166596	−0.001222
	0.1	0.232932	0.087075	0.059482	0.023744	0.302719	0.026602	0.024268	0.013437	1.525364	0.216033	0.131687	−0.041922
	0.2	0.264702	0.077224	0.052219	0.030204	0.33387	0.029038	0.026208	0.016248	1.615305	0.166618	0.103641	−0.067664
	0.3	0.294775	0.067789	0.045046	0.036181	0.357122	0.030870	0.027704	0.018388	1.690332	0.128725	0.079327	−0.085726
	0.4	0.323652	0.058776	0.037981	0.041714	0.376151	0.032386	0.028971	0.020124	1.755706	0.098128	0.057874	−0.098972
	0.5	0.351586	0.050152	0.031043	0.046867	0.392475	0.033696	0.030086	0.021587	1.814088	0.072617	0.038749	−0.109008
	0.6	0.378733	0.041876	0.024239	0.051699	0.406881	0.034858	0.031090	0.022850	1.867088	0.050841	0.021549	−0.116818
	0.7	0.405204	0.033909	0.017571	0.056262	0.419840	0.035908	0.032008	0.023962	1.915779	0.031920	0.005967	−0.123038
	0.8	0.431082	0.026218	0.011037	0.060598	0.431660	0.036868	0.032855	0.024956	1.960923	0.015240	0.008245	−0.128092
	0.9	0.456431	0.018771	0.004631	0.064741	0.442554	0.037756	0.033644	0.025854	2.003084	0.000359	−0.021287	−0.132274
	1.0	0.481305	0.011544	0.001651	0.068718	0.452680	0.038582	0.034383	0.026674	2.042693	−0.013043	−0.033318	−0.135791

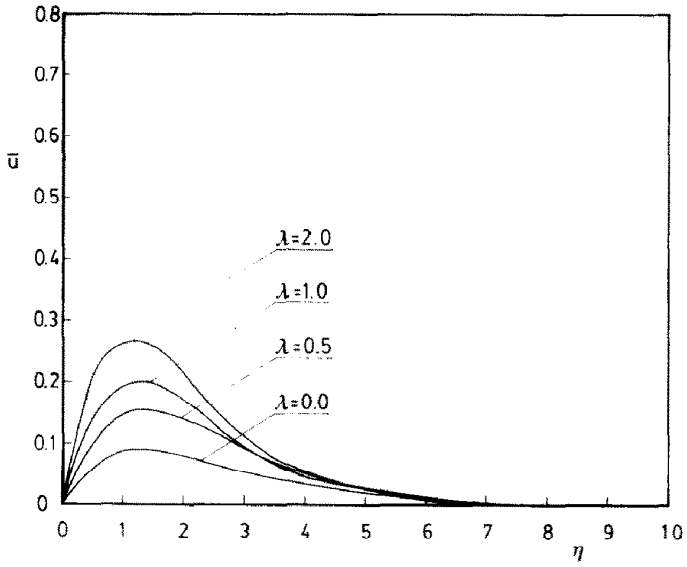

FIG. 2(a). Dimensionless transversal velocity profile $\bar{u}$ at $\bar{x} = \pi/6$ for various values of λ.

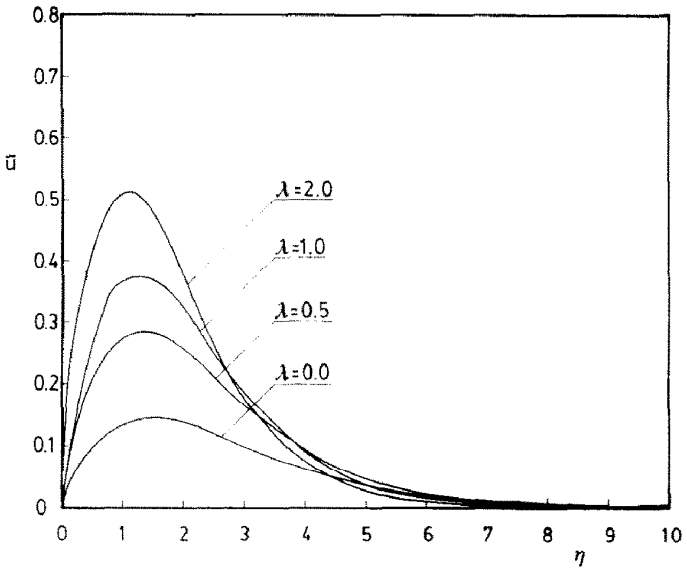

FIG. 2(b). Dimensionless transversal velocity profile $\bar{u}$ at $\bar{x} = \pi/3$ for various values of λ.

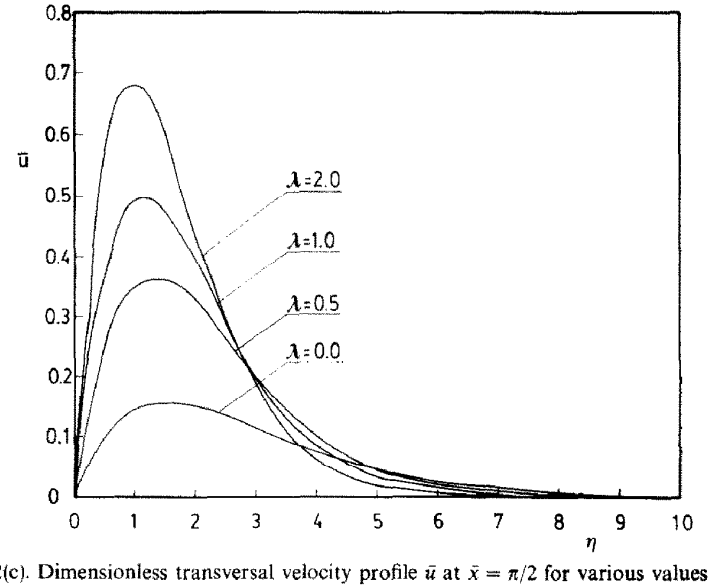

FIG. 2(c). Dimensionless transversal velocity profile $\bar{u}$ at $\bar{x} = \pi/2$ for various values of λ.

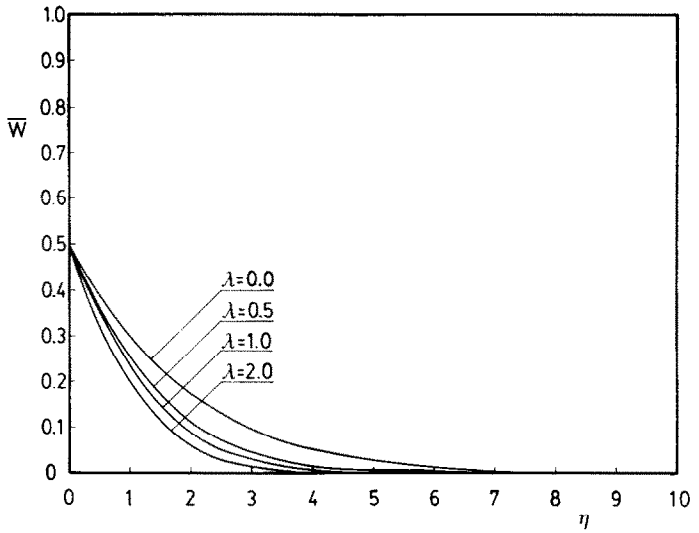

FIG. 3(a). Dimensionless circumferential velocity profile $\bar{\omega}$ at $\bar{x} = \pi/6$ for various values of λ.

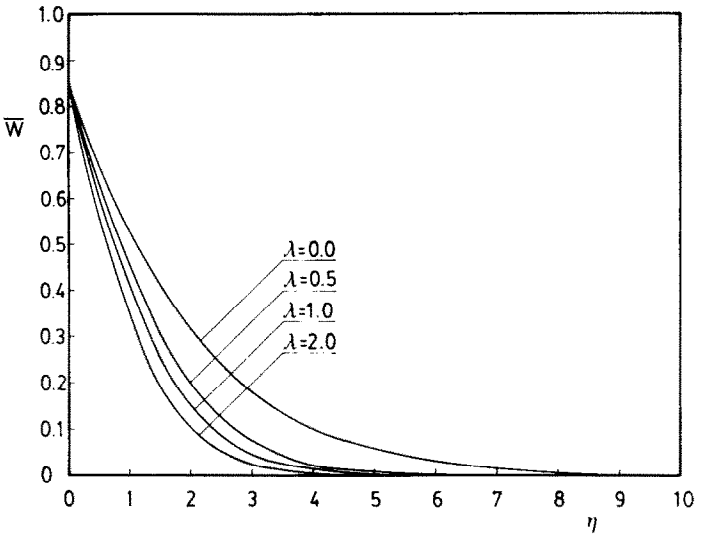

FIG. 3(b). Dimensionless circumferential velocity profile $\bar{\omega}$ at $\bar{x} = \pi/3$ for various values of λ.

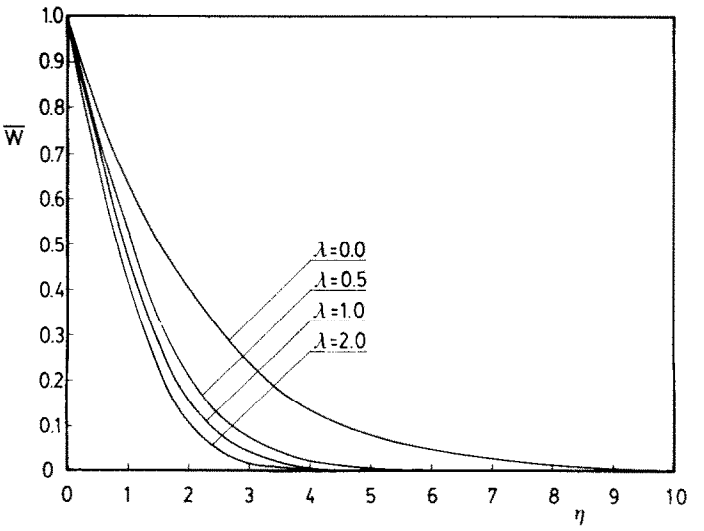

FIG. 3(c). Dimensionless circumferential velocity profile $\bar{\omega}$ at $\bar{x} = \pi/2$ for various values of λ.

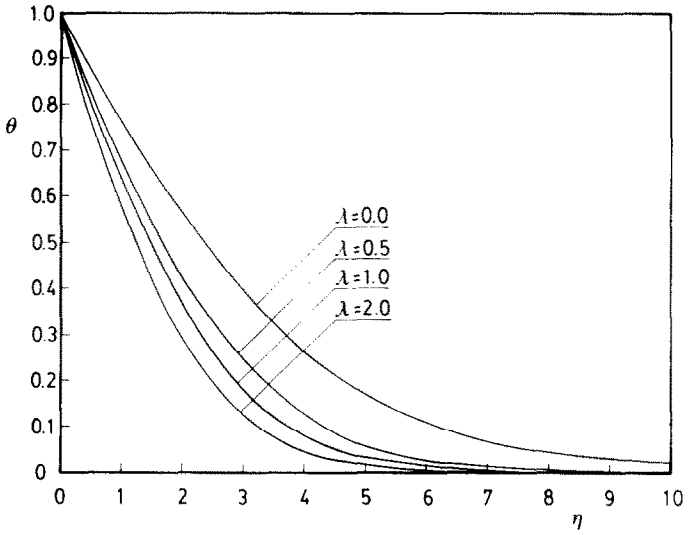

FIG. 4(a). Dimensionless temperature profile θ at $\bar{x} = \pi/6$ for various values of λ.

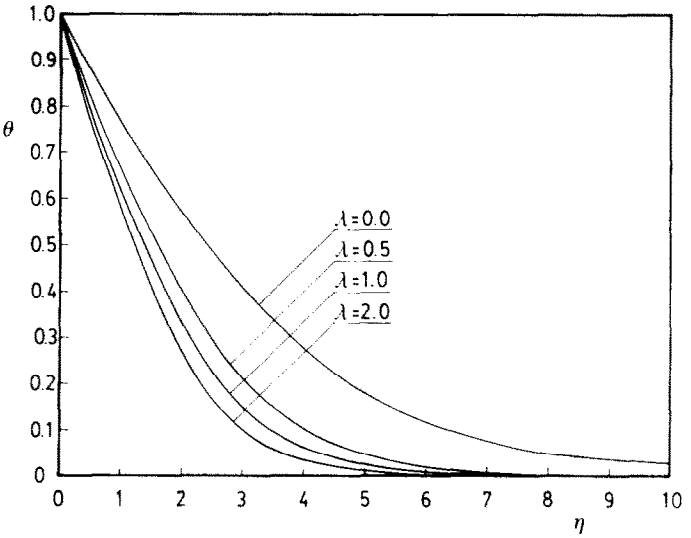

FIG. 4(b). Dimensionless temperature profile θ at $\bar{x} = \pi/3$ for various values of λ.

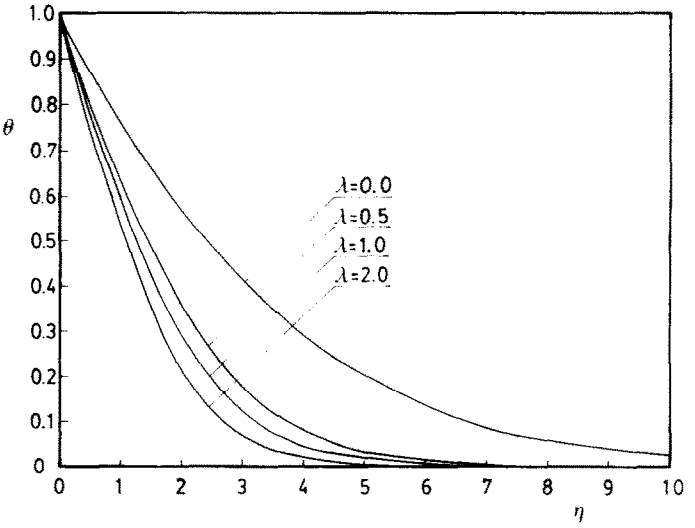

FIG. 4(c). Dimensionless temperature profile θ at $\bar{x} = \pi/2$ for various values of λ.

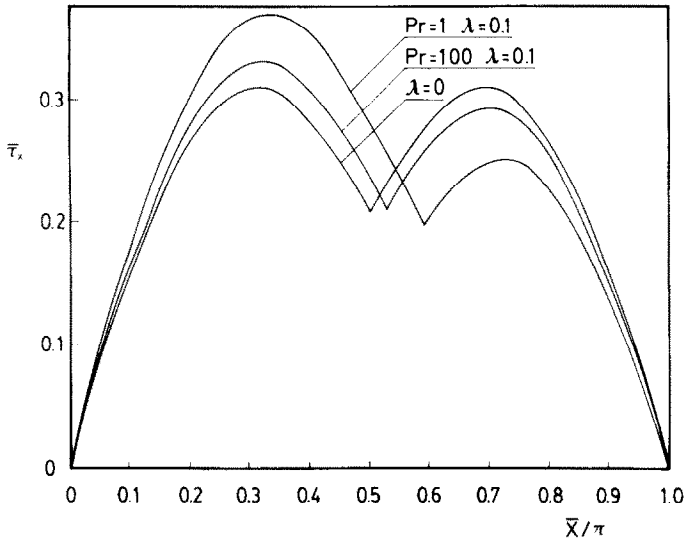

FIG. 5. Dimensionless x-component of local wall friction on a sphere surface.

Having known the validity region for application of the results obtained in analyzing the buoyancy force effects on a rotating hemisphere, the local Nusselt numbers can now be determined and these are shown in Fig. 6. If x_r denotes the eruption point, the torque due to the friction force can be calculated from

$$\bar{M} = \frac{MRe^{1/2}}{\rho R^4 \omega^2} = 2\pi\left[\int_0^{\bar{x}_r} \bar{r}^2 \tau_z|_\lambda \mathrm{d}\bar{x} + \int_0^{\pi-\bar{x}_r} \bar{r}^2 \bar{\tau}_z|_{-\lambda} \mathrm{d}\bar{x}\right] \tag{64}$$

and similarly, the total heat transfer from the sphere surface is

$$Q = 2\pi R^2\left[\int_0^{\bar{x}_r} \bar{r}^2 q|_\lambda \mathrm{d}\bar{x} + \int_0^{\pi-\bar{x}_r} \bar{r}^2 q|_{-\lambda} \mathrm{d}\bar{x}\right]. \tag{65}$$

For the case where λ is sufficiently large, it is possible that the separation occurs not due to the collision of flow but due to the vanishing of the local shear stress at the wall. In this case the equation (64) cannot be applied without further analysis.

6. CONCLUSIONS

In this paper, the effects of buoyancy force on laminar flow and heat transfer over rotating axisymmetric round-nosed bodies are analysed by employing a Görtler type series of solutions. As an example, the series have been applied to the case of rotating hemispheres and using these results the buoyancy-force effects on a rotating sphere are examined, including the effects on the eruption of flow due to geometrical symmetry of the spheres. From the obser-

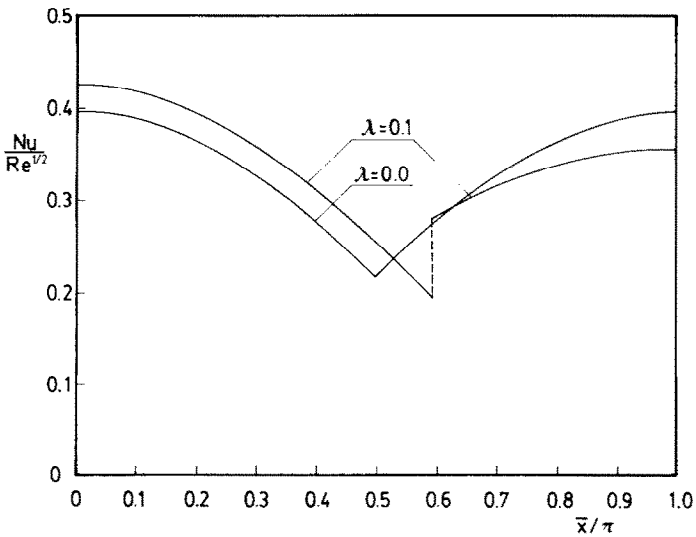

FIG. 6(a). Local Nusselt number on a sphere surface for $\lambda = 0.1$ and $Pr = 0.72$.

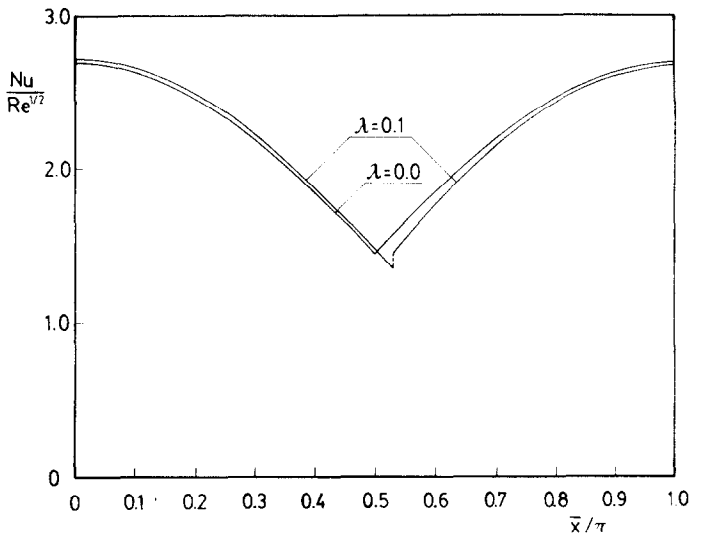

FIG. 6(b). Local Nusselt number on a sphere surface for $\lambda = 0.1$ and $Pr = 100$.

vation of the numerical results for rotating hemispheres, it is seen that the effects of buoyancy force are more significant for flow engendered by rotating bodies than for flows over submerged bodies.

Acknowledgements — The author gratefully acknowledges the support for this work from the Alexander von Humboldt Foundation through special funds given during author's stay in Germany.

REFERENCES

1. E. M. Sparrow and J. L. Gregg, Buoyancy effects in forced convection flow and heat transfer, *J. Appl. Mech.* **81**, 133–134 (1959).
2. A. A. Szewezyk, Combined forced and free convection laminar flow, *J. Heat Transfer* **86**, 501–507 (1964).
3. J. H. Merkin, The effect of buoyancy forces on the boundary layer flow over a semi-infinite vertical flat plate in a uniform free stream, *J. Fluid Mech.* **35**, 439–450 (1969).
4. J. R. Lloyd and E. M. Sparrow, Combined forced and free convection flow on vertical surfaces, *Int. J. Heat Mass Transfer* **13**, 434–438 (1970).
5. B. Gebhart and L. Pera, Mixed convection from long horizontal cylinders, *J. Fluid Mech.* **45**, 49–64 (1971).
6. T. S. Chen and A. Mucoglu, Buoyancy effects on forced convection along a vertical cylinder, *J. Heat Transfer* **97**, 198–203 (1975).
7. P. H. Oosthuizen and S. Madan, Combined convective heat transfer from horizontal cylinder in air, *J. Heat Transfer* **92**, 194–196 (1970).
8. G. Wilks, Heat transfer coefficients for combined forced and free convection flow about a semi-infinite isothermal plate, *Int. J. Heat Mass Transfer* **19**, 951–953 (1976).
9. F. Kreith, Convection heat transfer in rotating system, *Adv. Heat Transfer* **5**, 129–251 (1968).
10. W. H. H. Banks, The laminar boundary layer on a rotating sphere, *Q. J. Mech. Appl. Math.* **18**, 443–454 (1965).
11. W. H. H. Banks, The thermal laminar boundary layer on a rotating sphere, *Z. Angew. Math. Phys.* **16**, 780–788 (1965).
12. D. R. Jeng, K. J. De Wit and M. H. Lee, Forced convection over rotating bodies with non-uniform surface temperature, *Int. J. Heat Mass Transfer* **22**, 89–97 (1979).
13. F. Kreith, L. G. Roberts, J. A. Sullivan and S. N. Sinha, Convection heat transfer and flow phenomena of rotating spheres, *Int. J. Heat Mass Transfer* **6**, 881–895 (1963).
14. L. A. Dorfman and A. Z. Serazetdinov, Laminar flow and heat transfer near rotating axisymmetric surface, *Int. J. Heat Mass Transfer* **8**, 317–327 (1965).
15. L. A. Dorfman and V. A. Mironova, Solution of equations for the thermal boundary layer at rotating axisymmetric surface, *Int. J. Heat Mass Transfer* **13**, 81–92 (1970).
16. A. Suwono, Laminar boundary layer flows near rotating bodies of arbitrary contour, *J. Fluids Engng* (submitted).
17. A. Suwono, Heat transfer from rotating bodies of arbitrary contour, *J. Heat Transfer* (in press).
arbitrary contour, *J. Heat Transfer* (in press).
18. F. N. Lin and B. T. Chao, Laminar free convection over two-dimensional and axisymmetric bodies of arbitrary contour, *J. Heat Transfer* **96**, 435–442 (1974).
19. D. A. Saville and S. W. Churchill, Laminar free convection in boundary layers near horizontal cylinders and vertical axisymmetric bodies, *J. Fluid Mech.* **29**, 391–399 (1967).

EFFETS DE LA GRAVITATION SUR L'ECOULEMENT ET LE TRANSFERT DE CHALEUR SUR DES CORPS RONDS AXISYMMETRIES TOURNANTS

Résumé — On etudie théoriquement l'écoulement et le transfert de chaleur en regime laminair permament sur des corps ronds axisymmetries tournants en tenant compte les effets de la gravitation. Les solutions des équations gouvernant l'écoulement et le transfert de chaleur sont données sous formes de séries. Les calculs numeriques sont faites pour les hemisphères tournantes, pour $\lambda = Gr/Re^2$ varie entre 0 et ∞ et les nombres de Prandtl $Pr = 0.72$ et 100. Pour le cas d'ecoulement opposant, les resultats numeriques sont donnés seulement pour λ petits. En utilisant ces résultats, on etudie également les effets de la gravitation sur l'écoulement et le transfert de chaleur sur une sphère tournante y compris les effets sur éruption d'écoulement.

AUFTRIEBSWIRKUNG AUF STRÖMUNG UND WÄRMESTROM AN ROTIERENDEN, ACHSENSYMMETRISCHEN KÖRPERN MIT ABGERUNDETER NASE

Zusammenfassung—Die Abhandlung beschreibt eine theoretische Untersuchung der ausgebildeten Laminarströmung und des Wärmeübergangs an rotierenden, achsensymmetrischen Körpern mit abgerundeter Nase, wobei Auftriebskräfte mit in Rechnung gestellt werden. Die Lösungen der Hauptgleichungen werden in Form von Reihenentwicklungen ausgedrückt. Die zahlenmäßigen Berechnungen wurden für den Fall von rotierenden Halbkugeln bei Lambda-Zahlen ($\lambda = Gr/Re^2$) im Bereich von Null bis unendlich und bei Prandtl-Zahlen (Pr) im Bereich von 0,72 bis 100 durchgeführt. Für den Fall entgegengerichteter Strömung werden die zahlenmäßigen Ergebnisse nur für kleine Werte von Lambda angegeben. Mit Hilfe der Ergebnisse, die bei der Halbkugel erhalten wurden, werden die Auftriebseinflüsse auf Strömung und Wärmestrom an einer Kugel unter Einschluß ihrer Wirkung auf die Strömungsablösung untersucht.

ВЛИЯНИЕ ПОДЪЕМНЫХ СИЛ НА ТЕЧЕНИЕ И ТЕПЛОПЕРЕНОС НА ВРАЩАЮЩИХСЯ ОСЕСИММЕТРИЧНЫХ ТЕЛАХ С КРУГЛОЙ НОСОВОЙ ЧАСТЬЮ

Аннотация — Проведен теоретический анализ стационарного ламинарного течения и теплопереноса на вращающихся осесимметричных телах с учетом влияния подъемных сил. Основные уравнения решены с помощью разложения в ряд. Получены численные решения для вращающихся полусфер при $\lambda = Gr/Re^2$ в диапазоне от 0 до ∞ и при значениях числа Прандтля, равных 0,72 и 100. Для случая встречного течения численные решения представлены только для малых значений λ. На основании результатов, полученных для полусфер, исследовалось влияние подъемных сил на течение и теплоперенос около сферы, а также на срыв потока.